GEOPHYSICAL RESEARCH LETTERS, VOL. 36, L07809, doi:10.1029/2008GL036779, 2009

Shifting the diurnal cycle of parameterized deep convection over land

C. Rio,[1] F. Hourdin,[1] J.-Y. Grandpeix,[1] and J.-P. Lafore[2]

Received 4 December 2008; revised 6 February 2009; accepted 13 February 2009; published 14 April 2009.

[1] In most atmospheric circulation models used for climate projections, cloud and convective processes are not explicitly resolved but parameterized. Such models are known to produce a diurnal cycle of continental thunderstorms in phase with insolation, while observed precipitation peaks in late afternoon. We propose a new approach which corrects this long standing bias of parameterized convection. In this approach, deep convection triggering and intensity are controlled by sub-cloud processes: here boundary layer thermals and gust fronts, and potentially orography or surface heterogeneities. The representation of the diurnal cycle of deep convection is greatly improved in 1D mode, with rainfall maximum delayed from midday to late afternoon, provided parameterizations account for the key role played by shallow cumulus in preconditioning deep convection and by gust fronts in the self-sustaining of thunderstorms in the afternoon. **Citation:** Rio, C., F. Hourdin, J.-Y. Grandpeix, and J.-P. Lafore (2009), Shifting the diurnal cycle of parameterized deep convection over land, *Geophys. Res. Lett.*, *36*, L07809, doi:10.1029/2008GL036779.

1. Introduction

[2] In current climate models, with typical resolution of 30 to 300 km, convective and cloud processes are subgrid-scale and must be "parameterized", i.e. represented through a set of approximate equations describing their ensemble behaviour and their effect on the large-scale variables. Models with parameterized convection are known to produce a diurnal cycle of continental thunderstorms in phase with insolation [*Betts and Jakob*, 2002; *Guichard et al.*, 2004], while observed precipitation peaks in late afternoon [*Yang and Slingo*, 2001]. This erroneous response to the strong diurnal forcing as well as the huge dispersion in simulations of present day climatology and trends of tropical rainfall [*Intergovernmental Panel on Climate Change* (*IPCC*), 2007] have brought into question the use of parameterized convection in climate change simulations. Given the foreseen computer evolution, running series of long climate change simulations with a resolution fine enough to explicitly resolve the largest convective structures (1–2 km) will however not be feasible within a couple of decades. To increase confidence in climate change simulations, it is worth improving further the physical content of climate models and in particular the representation of convective clouds.

[3] Atmospheric convection can be either shallow or deep depending on dominant physical processes and dynamical regimes. Shallow convection is associated with organized boundary layer structures (cells, rolls, ...) and is driven by surface heat flux and entrainment at boundary layer top. Shallow cumulus, with a vertical extension of a few kilometres, may be seen as the saturated part of plumes of warm air, called thermals, originating from the surface and driven by buoyancy [*LeMone and Pennell*, 1976]. They contribute to the preconditioning of deeper convection, through a gradual deepening of the boundary layer and moistening of the inversion layer [*Chaboureau et al.*, 2004; *Stevens*, 2006]. Deep cumulonimbus convection bursts locally overcoming an inhibition barrier located at the boundary layer top and is mainly driven by water phase changes. Evaporation of rainfall under deep convective clouds generates pools of cold air, also called density currents or wakes, the spreading edges of which form gust fronts which lift the air and initiate new convection [*Lima and Wilson*, 2008].

[4] While some recent studies encourage the development of unified convection schemes [*Kuang and Bretherton*, 2006], we present here a new approach based on a distinct treatment of shallow and deep convection. This choice allows us to represent the control of deep convection initiation and maintenance by sub-cloud processes – here thermals and wakes (see illustration in Figure 1).

2. Deep Convection Controlled by Sub-cloud Processes

[5] To capture the diurnal cycle of convection, it is essential to represent the succession of three regimes of convection: dry, moist non-precipitating, precipitating.

[6] For boundary layer turbulence and shallow convection, we combine a diffusive approach for small-scale turbulence based on a prognostic equation for the turbulent kinetic energy [*Yamada*, 1983] with a mass-flux scheme that represents the vertical transport by thermals within the convective boundary layer [*Hourdin et al.*, 2002; *Coindreau et al.*, 2007; *Rio and Hourdin*, 2008]. Coherent structures within a horizontal grid cell of a large-scale model are idealized by considering a mean ascending dry or cumulus toped thermal of mass-flux f, surrounded by subsidence in the environment of mass-flux $-f$. The fractional area α_u covered by the plume, the plume vertical velocity w_u and the mass-flux $f = \alpha_u \rho w_u$, ρ being the air density, are computed from mass conservation:

$$\frac{\partial f}{\partial z} = e - d \tag{1}$$

[1] Laboratoire de Météorologie Dynamique, Université Paris 6, Paris, France.
[2] Centre National de Recherches Météorologiques, GAME, Météo-France, CNRS, Toulouse, France.

0094-8276/09/2008GL036779$05.00

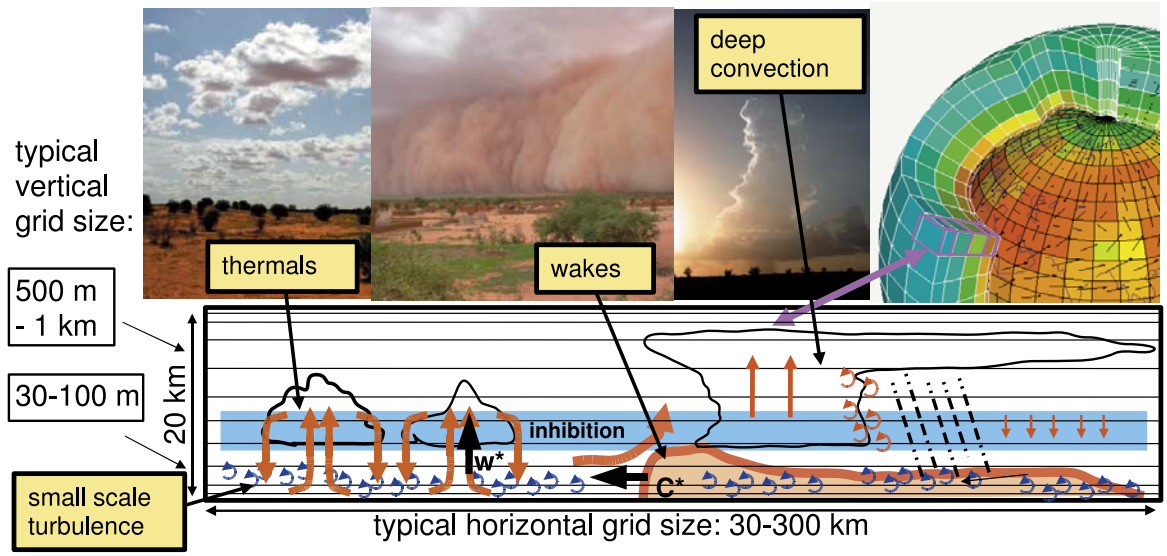

Figure 1. Sketch of physical processes accounted for within a model grid cell illustrated with clouds pictures taken by Françoise Guichard. Three scales of motion are distinguished: small scale eddies, coherent structures of the convective boundary layer, and deep convection associated with precipitation and wakes. The thermals (of maximal vertical velocity w_*) and wake gust fronts (of speed C_*) provide energy to overcome the inhibition at the top of the boundary layer and power to uplift a given air-mass at the base of deep convective clouds.

(e and d being the entrainment and detrainment rates respectively), and from the equation of vertical momentum in stationary and frictionless conditions:

$$\frac{\partial f w_u}{\partial z} = -d w_u + \alpha_u g \rho \frac{\theta_{vu} - \overline{\theta_v}}{\overline{\theta_v}} \quad (2)$$

where θ_{vu} (respectively $\overline{\theta_v}$) is the plume (respectively large-scale) virtual potential temperature. The closure of the scheme relates the mass-flux at the base of the thermal plume to the instability of the surface layer (see details given by *Rio and Hourdin* [2008] and auxiliary material).[1] Boundary layer convection and shallow clouds are represented in a unified way, with no discontinuity at cloud base. The so-called "thermal plume model" used here and similar approaches [*Soares et al.*, 2004; *Siebesma et al.*, 2007] were shown to effectively reproduce the diurnal cycle of the continental boundary layer on fair-weather cumulus days.

[7] The transition from shallow to deep convection is handled by coupling the thermal plume model with a deep convection scheme derived from *Emanuel* [1991], which triggering function and closure have been modified in order to relate them to sub-cloud processes. Deep convection is initiated as soon as the kinetic energy of parcels inside thermals, called the Available Lifting Energy (ALE = $\mathrm{ALE^{th}} = w_*^2/2$ in J kg^{-1}) overcomes the Convective INhibition (CIN), so that deep convection is active when:

$$ALE > |\mathrm{CIN}| \quad (3)$$

Considering an air parcel rising adiabatically from the surface; the CIN is defined as the work of buoyancy forces in the region of negative buoyancy, around cloud base. The work of positive buoyancy forces above is called the Convective Available Potential Energy (CAPE). Here, w_* is the maximal of w_u on the vertical, which corresponds at transition time to the vertical velocity near the top of shallow clouds. A similar criteria was used by *Bretherton et al.* [2004] for shallow convection triggering using a typical vertical velocity at cloud base.

[8] The flux of kinetic energy associated with thermals defines the Available Lifting Power (ALP, in W m^{-2}) which is used to determine the convective intensity through a new ALP-closure. The convective power above inhibition $\frac{1}{2}M_b w_b^2$ – where M_b is the deep convective mass-flux and w_b the vertical velocity at level of free convection taken as a constant of 1 m s^{-1} at this stage – is computed as:

$$\frac{1}{2}M_b {w_b}^2 = ALP - M_b\left[|CIN| + \gamma w_b^2\right] \quad (4)$$

where M_b $|CIN|$ is the power consumed to overcome inhibition and the last term is the power lost by dissipation (assumed to scale with $M_b w_b^2$). The power provided by thermals is taken as $\mathrm{ALP^{th}} = k_{th}\rho\overline{w'^3}/2$ where the third order moment of the vertical velocity reads $\overline{w'^3} = \frac{\alpha_u(1-2\alpha_u)}{(1-\alpha_u)^2} w_u^3$ and k_{th} is an adjustable parameter.

[9] After deep convection initiation, evaporation of precipitation generates cold pools represented here by the wake parameterization described in the auxiliary material. Each atmospheric column is divided into a mean wake and its environment. The wake fractional cover within the grid cell evolves according to the wake spread rate C_* which depends on the Wake Available Potential Energy, $C_* = k_*\sqrt{2\mathrm{WAPE}}$, with

$$\mathrm{WAPE} = -g\int_0^{h_w} \frac{\delta\theta_v}{\overline{\theta_v}} dz \quad (5)$$

where h_w is the height of wakes and k_* is an adjustable parameter. The difference of virtual potential temperature

[1] Auxiliary materials are available in the HTML. doi:10.1029/2008GL036779.

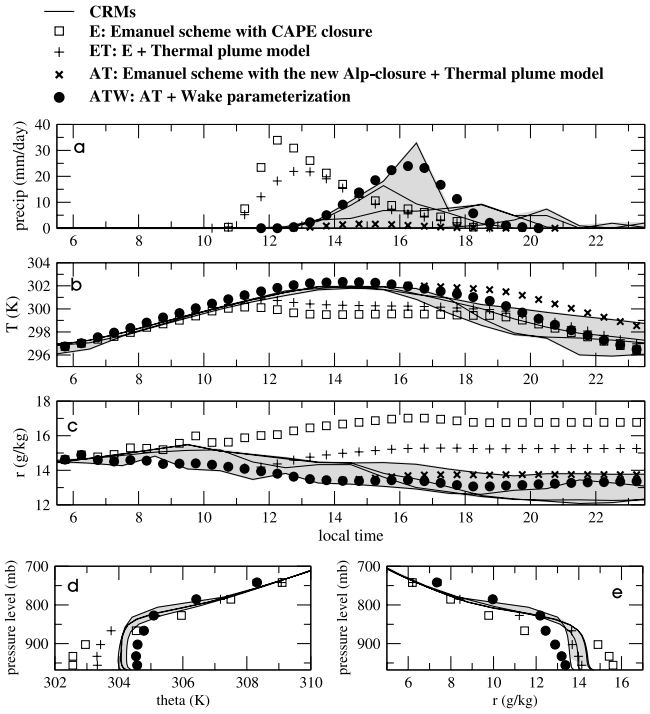

Figure 2. Simulations of the diurnal cycle for the EUROCS case. (a) Diurnal evolution of precipitation (mm day^{-1}), (b) temperature (K) and (c) specific humidity (g. kg^{-1}) in the first model layer, and (d) vertical profiles of potential temperature (K) and (e) specific humidity (g. kg^{-1}) at 12:30LT for the EUROCS case study. Results are shown for the single column version of LMDZ with various combinations of convection schemes (simulations E, ET, AT and ATW) and three CRMs simulations from *Guichard et al.* [2004] (MESO-NH [*Lafore et al.*, 1998], CRCP [*Grabowski and Smolarkiewicz*, 1999] and UKLEM [*Schutts and Gray*, 1994] with two different resolutions, light dark lines). The shaded area corresponds to the envelope of the CRMs results. Note that as the wake parameterization is only active after precipitation onset, simulations AT and ATW are identical until 13:00 LT.

between the wake and its environment, $\delta\theta_v$, is driven to first order by reevaporation of convective rainfall in the unsaturated downdraughts of the Emanuel's scheme, supposed to take place inside wakes. Gust fronts associated with wakes provide an additional lifting energy $ALE^{wk} \simeq C_*^2$ which maintains convection active even after thermals extinction (as long as $\max(ALE^{th}, ALE^{wk}) > |CIN|$), and an additional lifting power $ALP^{wk} \simeq C_*^3$, $ALP = ALP^{th} + ALP^{wk}$ being used in the ALP-closure (see details and parameters values in the auxiliary material).

[10] While closures for deep convection classically rely on large-scale variables either through the CAPE [*Emanuel*, 1991]), horizontal moisture convergence [*Tiedtke*, 1989] or temperature and humidity profiles below clouds [*Emanuel and Zivkovic-Rothman*, 1999], the ALE and ALP concepts introduced here allow to account for the role played on deep convection development by cloud base layer [*Chaboureau et al.*, 2004] or tropospheric [*Derbyshire et al.*, 2004] humidity, by the size of thermals at cloud base [*Kuang and Bretherton*, 2006], and by wakes [*Khairoutdinov and Randall*, 2006].

3. Diurnal Cycle of Convection Over Land

3.1. Diurnal Cycle of Convection on the EUROCS Case

[11] We use, for evaluation purposes, the idealized EUROCS case [*Guichard et al.*, 2004], built from observations collected over the Southern Great Plains (USA) at the Atmospheric Radiation Measurement site between the 27th and 30th of June 1997. The case is defined by initial conditions, large-scale forcings and sensible and latent heat fluxes having a maximum around midday of 120 W m^{-2} and 400 W m^{-2} respectively.

[12] *Guichard et al.* [2004] compare large-scale models in single-column mode with Cloud Resolving Models (CRMs) run on a horizontal domain corresponding to a typical grid cell of global models. CRMs succeed in simulating the observed transition from shallow cumulus in the morning to deep convection in the afternoon on that case despite a too coarse resolution (250 m to 2 km) to resolve explicitly boundary layer circulations. Parameterized convective precipitation starts around 09:00LT instead of 12:00LT, illustrating that the bias of full 3D large-scale models is reproduced when models are used in a single-column mode.

[13] Following the same approach, CRMs are used here to evaluate various combinations of the parameterizations presented above in the 1-dimensional version of the LMDz model (the atmospheric component of one of the IPCC global climate models [*Hourdin*, 2006; *IPCC*, 2007]) run with a vertical resolution of 31 layers for the entire atmospheric column and a 5-minute time-step starting from 5:30LT. Figure 2a displays the diurnal evolution of precip-

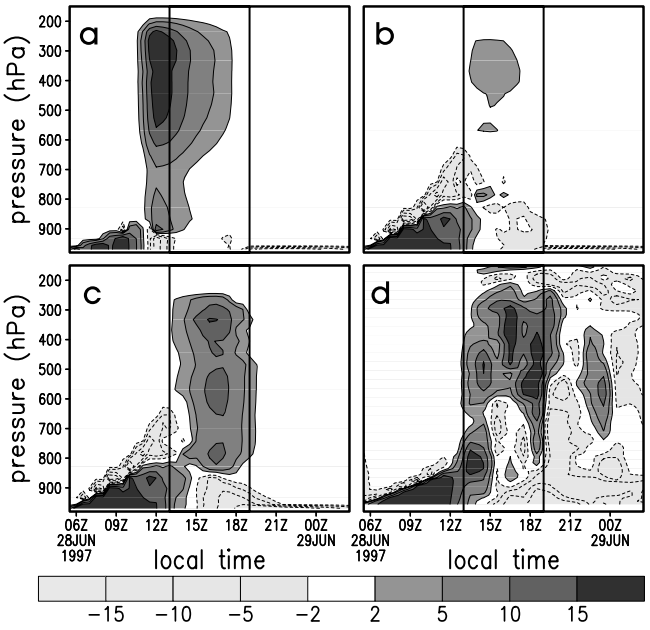

Figure 3. Simulations of atmospheric heating by convective processes. Apparent heat source Q_1 (K day^{-1}) associated with turbulence, shallow and deep convection: results obtained with simulations (a) E, (b) AT, (c) ATW, and (d) MESO-NH in a CRM mode.

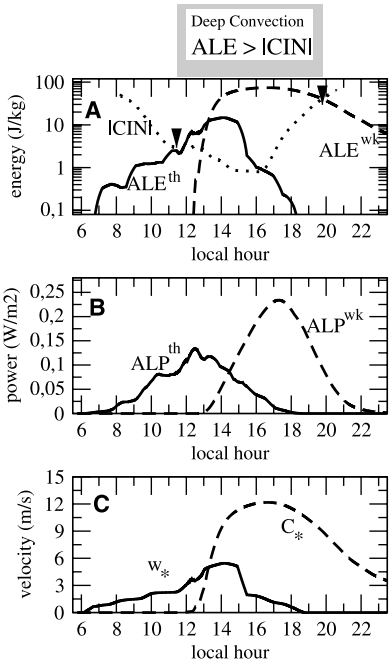

Figure 4. Diurnal cycle of available lifting energy and power for the EUROCS case. Diurnal evolution of (a) the Available Lifting Energy and Convective INhibition (ALE & CIN, J. kg^{-1}), (b) the Available Lifting Power (W. m^{-2}) provided by thermals (dark line) and wakes (dashed line) and (c) w_* (m s^{-1}, dark line) and C_* (m s^{-1}, dashed line) for simulation ATW.

itation obtained with the various simulations and CRMs from *Guichard et al.* [2004]. With a classical diffusive approach for boundary layer turbulence and the original CAPE closure version of the Emanuel scheme (simulation E), rain starts too early by about 2 hours and peaks 4 hours too early compared with CRMs. Activation of the Thermal plume model (simulation ET) does not change the onset time but delays the maximum rainfall by one hour. When controlling convection by the thermal plume model with the new ALE and ALP concepts (simulation AT), the onset of precipitation is delayed from 11:00LT to 13:00LT, in much better agreement with CRMs, but precipitation is much too weak. Activation of the wake parameterization (simulation ATW) allows a gradual reinforcement of precipitation in the afternoon, resulting in both good phasing and intensity when compared with CRMs.

[14] How can we explain this phase shift?

3.2. Deep Convection Preconditioning

[15] Compared with the original simulation (simulation E), activation of the thermal plume model (simulation ET) results in a faster deepening boundary layer in the morning, with stronger heating in the mixed layer and cooling at the inversion as seen from the comparison of the convective (shallow plus deep) apparent heat source Q_1 (Figure 3). As a consequence, the air is warmer and drier near surface (Figures 2b and 2c), due to a stronger mixing with tropospheric air via the compensating subsidence. Around midday, at a time close to deep convection initiation, the air is consequently moister and colder in the inversion layer (Figures 2d and 2e).

[16] The thermal plume model, by a better representation of boundary layer processes, thus allows a better preconditioning for deep convection: a larger inhibition, and a gradual moistening of the inversion layer by cumulus clouds. This is not enough however to delay convection with the old convection scheme. With the new scheme (simulations AT and ATW), deep convection is delayed until CIN is overcome by the thermals kinetic energy, ALE^{th} (Figure 4a), deduced from w_* (Figure 4c), which increases suddenly around midday, when the latent heat release associated with condensation in thermals is strong enough to make the vertical velocity increase from cloud base to cloud top. Convection then suddenly switches from shallow to deep.

3.3. Deep Convection Continuation

[17] The further evolution of convection in the afternoon is governed by several feedbacks. On the one hand, precipitating downdraughts cool the boundary layer and dry the inversion, inhibiting the formation of thermals and cumulus clouds, in turn weakening deep convection which vanishes after thermal extinction in simulation AT (Figure 3b). On the other hand, gust fronts associated with wakes reinforce convection. The additional lifting energy provided by wakes (simulation ATW; Figure 4a), deduced from C_* (Figure 4c), keeps deep convection active until 20:00LT, while the additional lifting power (Figure 4b) intensifies deep convection, with an apparent heat source Q_1 comparable with CRM results (Figures 3c and 3d). This yields colder air at the surface in the evening, in better agreement with CRMs (Figure 2b).

4. Conclusion

[18] We have shown with a single-column version of the general circulation model LMDz that it is finally possible to simulate a realistic diurnal cycle of convective rainfall with parameterized convection. In the present approach, thermals drive shallow convection in the morning and play a key role in the preconditioning and triggering of deep convection while wakes reinforce thunderstorms in late afternoon. The control of deep convection by boundary layer processes relies on the new ALE and ALP concepts, at first designed to couple the wake and deep convection parameterizations. Those concepts may also be used to account for other factors such as thermal breezes along orography slopes or land-sea contrasts.

[19] The set of parameterizations presented here is at the heart of the future version of LMDz, the atmospheric component of the IPSLCM4 climate model [*Braconnot et al.*, 2007] used for climate change projections in the frame of IPCC. Hopefully it will help obtain realistic present climatology and variability of tropical rainfall and improve confidence in its evolution in climate projections, a key issue for impact studies of global warming on human societies.

[20] **Acknowledgments.** The authors want to thank Françoise Guichard for providing CRMs results on the EUROCS case and Pascal Marquet and Marie-Pierre Lefèbvre for providing the case set up. We also thank Laurent Fairhead and Jean-Louis Dufresne for useful comments on the manuscript, as well as Praveen Kumar and two anonymous reviewers. Figures and graphs were made using grads and xmgrace free softwares.

References

Betts, A. K., and C. Jakob (2002), Study of diurnal cycle of convective precipitation over Amazonia using a single column model, *J. Geophys. Res.*, *107*(D23), 4732, doi:10.1029/2002JD002264.

Braconnot, P., F. Hourdin, S. Bony, J.-L. Dufresne, J.-Y. Grandpeix, and O. Marti (2007), Impact of different convective cloud schemes on the simulation of the tropical seasonal cycle in a coupled ocean-atmosphere model, *Clim. Dyn.*, *29*, 501–520.

Bretherton, C., J. McCaa, and H. Grenier (2004), A new parameterization for shallow cumulus convection and its application to marine subtropical cloud-topped boundary layers. Part I: Description and 1D results, *Mon. Weather Rev.*, *132*, 864–882.

Chaboureau, J.-P., F. Guichard, J.-L. Redelsperger, and J.-P. Lafore (2004), The role of stability and moisture in the diurnal cycle of convection over land, *Q. J. R. Meteorol. Soc.*, *130*, 3105–3117.

Coindreau, O., F. Hourdin, M. Haeffelin, A. Mathieu, and C. Rio (2007), Assessment of physical parameterizations using a global climate model with stretchable grid and nudging, *Mon. Weather Rev.*, *135*, 1474–1489.

Derbyshire, S. H., I. Beau, P. Bechtold, J.-Y. Gandpeix, J.-M. Piriou, J.-L. Redelsperger, and P. Soares (2004), Sensitivity of moist convection to environmental humidity, *Q. J. R. Meteorol. Soc.*, *130*, 3055–3079.

Emanuel, K. A. (1991), A scheme for representing cumulus convection in large-scale models, *J. Atmos. Sci.*, *48*, 2313–2335.

Emanuel, K. A., and M. Zivkovic-Rothman (1999), Development and evaluation of a convection scheme for use in climate models, *J. Atmos. Sci.*, *56*, 1766–1782.

Grabowski, W., and P. K. Smolarkiewicz (1999), CRCP: A cloud resolving convection parameterization for modeling the tropical convecting atmosphere, *Physica D*, *133*, 171–178.

Guichard, F., et al. (2004), Modelling the diurnal cycle of deep precipitating convection over land with cloud-resolving models and single column models, *Q. J. R. Meteorol. Soc.*, *130*, 3139–3172.

Hourdin, F., F. Couvreux, and L. Menut (2002), Parameterisation of the dry convective boundary layer based on a mass flux representation of thermals, *J. Atmos. Sci.*, *59*, 1105–1123.

Hourdin, F., et al. (2006), The LMDZ4 general circulation model: Climate performance and sensitivity to parametrized physics with emphasis on tropical convection, *Clim. Dyn.*, *27*, 787–813.

Intergovernmental Panel on Climate Change (IPCC) (2007), *Climate Change 2007: The Scientific Basis. Contribution of Working Group I to the Fourth Assessment Report of the Intergovernmental Panel on Climate Change*, edited by S. Solomon et al., 996 pp., Cambridge Univ. Press, Cambridge, U. K.

Khairoutdinov, M., and D. Randall (2006), High-resolution simulation of shallow-to-deep convection transition over land, *J. Atmos. Sci.*, *63*, 3421–3436.

Kuang, Z., and C. S. Bretherton (2006), A mass-flux scheme view of a high-resolution simulation of a transition from shallow to deep convection, *J. Atmos. Sci.*, *63*, 1895–1909.

Lafore, J.-P., et al. (1998), The Meso-NH atmospheric simulation system. Part I: Adiabatic formulation and control simulations, *Ann. Geophys.*, *16*, 90–109.

LeMone, M. A., and W. T. Pennell (1976), The relationship of trade wind cumulus distribution to subcloud layer fluxes and structure, *Mon. Weather Rev.*, *104*, 524–539.

Lima, M. A., and J. W. Wilson (2008), Convective storm initiation in a moist tropical environment, *Mon. Weather Rev.*, *136*, 1847–1864.

Rio, C., and F. Hourdin (2008), A thermal plume model for the convective boundary layer: Representation of cumulus clouds, *J. Atmos. Sci.*, *65*, 407–425.

Schutts, G. J., and M. E. B. Gray (1994), A numerical modelling study of the geostrophic adjustment process following deep convection, *Q. J. R. Meteorol. Soc.*, *120*, 1145–1178.

Siebesma, A., P. Soares, and J. Teixeira (2007), A combined eddy-diffusivity mass-flux approach for the convective boundary layer, *J. Atmos. Sci*, *64*, 1230–1248.

Soares, P., P. Miranda, A. Siebesma, and J. Teixeira (2004), An eddy-diffusivity/mass flux parameterization for dry and shallow cumulus convection, *Q. J. R. Meteorol. Soc.*, *130*, 3365–3383.

Stevens, B. (2006), On the growth of layers of non-precipitating cumulus convection, *J. Atmos. Sci.*, *64*, 2916–2931.

Tiedtke, M. (1989), A comprehensive mass flux scheme for cumulus parameterization in large-scale models, *Mon. Weather Rev.*, *117*, 1179–1800.

Yamada, T. (1983), Simulations of nocturnal drainage flows by a q^2l turbulence closure model, *J. Atmos. Sci.*, *40*, 91–106.

Yang, G. Y., and J. M. Slingo (2001), The diurnal cycle in the tropics, *Mon. Weather Rev.*, *129*, 784–801.

J.-Y. Grandpeix, F. Hourdin, and C. Rio, Laboratoire de Météorologie Dynamique, Université Paris 6, 4 place Jussieu, F-75005 Paris, France. (catherine.rio@lmd.jussieu.fr)

J.-P. Lafore, Centre National de Recherches Météorologiques, GAME, Météo-France, CNRS, 42 avenue Gaspard Coriolis, F-31057 Toulouse, France.